Mécanique & Industries 10, 195–201 (2009)
© AFM, EDP Sciences 2009
DOI: 10.1051/meca/2009065

www.mecanique-industries.org

Mécanique & Industries

A Combined analytical, experimental and numerical investigation of turbulent air flow behaviour in a rotor-stator cavity

Fadi Abdel Nour[1,a], Sébastien Poncet[2], Roger Debuchy[3] and Gérard Bois[1]

[1] PRES Université Nord de la France, Arts et Métiers ParisTech, 8, Boulevard Louis XIV, Laboratoire de Mécanique de Lille UMR CNRS 8107, 59046 Lille, France
[2] Laboratoire M2P2, UMR 6181 CNRS, Université d'Aix-Marseille, Technopôle Château-Gombert, 38 rue F. Joliot-Curie, 13451 Marseille, France
[3] PRES Université Nord de la France, IUT de Béthune, 1230 Rue de l'Université, Laboratoire de Mécanique de Lille UMR CNRS 8107, BP 819, 62408 Béthune, France

Received 20 April 2009

Abstract – The present work considers the turbulent air flow inside an annular high speed rotor-stator cavity opened to the atmosphere at the periphery, where the pre-swirl ratio of the fluid is low. The interdisk spacing is sufficiently large so that the boundary layers developed on each disk are separated and the flow belongs to the regime IV of Daily and Nece (ASME J. Basic Eng. 82 (1960) 217–232). In such a system, the solid body rotation of the core predicted by Batchelor (J. Mech. Appl. Math. 4 (1951) 29–41) in case of infinite disks is not always observed: the flow behaviour in the whole interdisk spacing is governed by the level of the pre-swirl velocity of the fluid which is closely linked to the peripheral geometry (Debuchy et al., Int. J. Rotating Machinery, (2007)). In the first part of the paper, experimental results performed by hot-wire probes introduced through the stator including mean radial and tangential velocity components, as well as three turbulent correlations, are presented for several peripheral boundary conditions leading to the same value of the pre-swirl ratio. In the second part, comparisons between experiments, numerical and analytical results are provided. The numerical approach is based on the Reynolds Stress Modeling (RSM) developed by Elena and Schiestel (Int. J. Heat Fluid Flow 17 (1996) 283–289). A good agreement between the different approaches is obtained for the mean and turbulent fields and especially for the distribution of the core swirl ratio.

Key words: Rotor-Stator cavity / analytical solution / hot-wire anemometry / RANS modeling

Résumé – Étude analytique, expérimentale et numérique du comportement d'un écoulement turbulent en air dans une cavité de type Rotor-Stator. Ce travail porte sur l'étude de l'écoulement turbulent en air à l'intérieur d'une cavité annulaire de type rotor-stator, ouverte à l'atmosphère en périphérie là où le taux de pré-rotation du fluide est faible. L'espace inter-disques est suffisamment important pour que les couches limites près des parois soient séparées, ce qui correspond au régime IV selon Daily et Nece (1960). Dans un tel système, on n'observe pas toujours la rotation en bloc du noyau central prévue par Batchelor (1951) dans le cas de disques infinis : le comportement de l'écoulement dans l'espace inter-disques est induit par le niveau de pré-rotation du fluide, lui-même étroitement lié à la géométrie périphérique du dispositif (Debuchy et al. 2007). Dans une première partie, on présente des résultats de mesures effectuées par sondes à fils chauds introduites au travers du stator, comprenant les composantes radiale et tangentielle de la vitesse moyenne ainsi que trois corrélations turbulentes, ceci pour différentes géométries périphériques conduisant toutes à la même valeur du taux de pré-rotation du fluide. Dans la deuxième partie, on effectue des comparaisons entre résultats expérimentaux, numériques et analytiques. L'approche numérique est basée sur le modèle de type Reynolds Stress Modeling (RSM) développé par Elena et Schiestel (1996). On obtient des résultats comparables pour les champs moyen et turbulent, et plus particulièrement pour l'évolution du taux de rotation du fluide dans le noyau central.

Mots clés : Cavité Rotor-Stator / solution analytique / anémométrie à fils chauds / modèle RANS

[a] Corresponding author: fadi_abdnour@hotmail.com

Article published by EDP Sciences

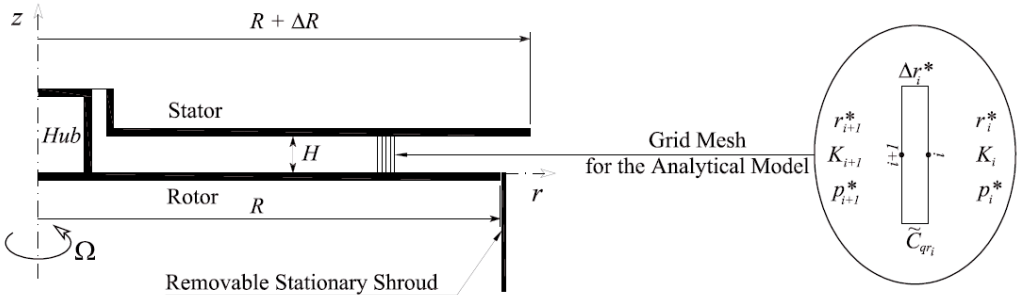

Fig. 1. Schematic representation of a rotor-stator cavity.

1 Introduction

Several and various researches have been carried out about turbulent flows inside rotor-stator cavities because of their relevance to the turbomachinery industry. As an example, the flow inside a rotor-stator cavity is a simplified geometrical configuration of a gas turbine cooling system. One historical controversy is due to Batchelor [1] who proposed a model based on the presence of a rotating core between the two boundary layers and Stewartson [2] who did not notice the solid rotation of the central core and the stator boundary layer. Later, it was found by Daily and Nece [3] that the flow structure can be divided into four regimes, laminar and turbulent, with or without separated boundary layers.

More recently, the flow inside enclosed systems has been the object of numerous experimental and numerical research programs. We can quote, among other studies, the experimental work of Itoh et al. [4], the numerical study of Elena and Schiestel [5] and the combined numerical and experimental investigations of Poncet [6] and Poncet et al. [7,8].

As far as opened rotor-stator system is concerned, the main supplementary difficulty comes from the high sensitivity of the flow properties to the geometrical configuration at the system periphery because of the interaction with the external domain. Djaoui et al. [9] introduced a geometrical parameter λ based on the possible difference between the disk radii and it was shown by Debuchy et al. [10] that the level of the pre-swirl velocity is closely linked to the variations of this parameter with the consequence that the Batchelor type flow is not always observed in a rotor-system without any superimposed flow.

The present work considers the air flow inside an annular high speed rotor-stator cavity belonging to the regime IV of Daily and Nece [3]: turbulent flow with separated boundary layers. The aim of this work is to provide comparisons between velocity measurements performed by hot-wire anemometry, numerical predictions of a second order turbulence modeling sensitized to rotation effects and an analytical solution.

2 Experimental set-up

The experimental apparatus consists of two parallel and coaxial disks separated by an adjustable interdisk space H (Fig. 1). The rotor and the central hub attached to it rotate at the same angular velocity Ω. For the test cases called "shrouded rotor system", the rotor was enclosed by a stationary shroud in order to minimize the perturbations brought by the centrifugal effects of the rotating walls external to the cavity. This stationary shroud was removed for the test case called "unshrouded rotor system". Two stators were tested: the "basic" one has the same radial dimension $R = 375$ mm as the rotor, whereas the other is slightly larger $R + \Delta R$. The present study focuses on the configuration where no superimposed centrifugal or centripetal inflows are assigned. The experiments were performed within air in ambient conditions [10].

In the present paper, H is fixed to 30 mm and Ω to 1500 rpm. Thus, the significant dimensionless parameters of the problem, which are the axial gap ratio of the cavity $G = H/R$ and the global Reynolds number $Re = \Omega R^2/\nu$ (ν the kinematic viscosity of the fluid), are fixed to 0.08 and 1.47×10^6 respectively. The combination of both parameters gives the Ekman number $Ek = (Re\,G^2)^{-1} = 1.06 \times 10^{-4}$. Two values of the geometrical parameter λ defined by $\lambda = \Delta R/H$ are tested: $\lambda = 0$ and $\lambda = 0.27$. r and z denote respectively the radial and axial coordinates : $r = 0$ at the axis and $z = 0$ on the rotating wall.

Radial (V_r) and tangential (V_θ) velocity components and the three associated turbulent correlations ($v_r'^2$, $v_\theta'^2$, $v_\theta' v_r'$) were measured with a specific hot-wire probe made of two perpendicular (5 μm) wires situated in the same plane. Each sensor was connected to a *DANTEC 55M25* anemometry device. For each measurement, 20000 samples were recorded with a data acquisition rate fixed to 10 kHz.

In the following discussion, all results are presented in dimensionless quantity form with superscript (*): $r^* = r/R$, $z^* = z/H$, $V_r^* = V_r/(\Omega r)$, $V_\theta^* = V_\theta/(\Omega r)$, $V_r'^{*2} = v_r'^2/(\Omega r)^2$, $V_\theta'^{*2} = v_\theta'^2/(\Omega r)^2$, $V_r'^* V_\theta'^* = v_r' v_\theta'/(\Omega r)^2$.

3 Statistical modeling

3.1 The differential Reynolds stress model (RSM)

The flow studied here presents several complexities (high rotation rate, wall effects, transition zones),

which are a severe test for turbulence modeling methods. Our approach is based on one-point statistical modeling using a low Reynolds number second-order full stress transport closure derived from the Launder and Tselepidakis [11] model and sensitized to rotation effects [5]. Poncet et al. [8] have shown that this level of closure was adequate in such flow configurations, while the usual k-ε model, which is blind to any rotation effect, presents serious deficiencies. This approach allows for a detailed description of near-wall turbulence and is free from any eddy viscosity hypothesis. The general equation for the Reynolds stress tensor R_{ij} can be written:

$$\dot{R}_{ij} = P_{ij} + D_{ij} + \Phi_{ij} - \varepsilon_{ij} + T_{ij} \tag{1}$$

where P_{ij}, D_{ij}, ϕ_{ij}, ε_{ij}, T_{ij} respectively denote the production, diffusion, pressure-strain correlation, dissipation and extra terms. The extra term T_{ij} accounts for implicit effects of the rotation on the turbulence field. It contains additional contributions in the pressure-strain correlation, a spectral jamming term, inhomogeneous effects and inverse flux due to rotation, which impedes the energy cascade.

3.2 Numerical method and boundary conditions

The computational procedure is based on a finite volume method using staggered grids for mean velocity components with axisymmetry hypothesis in the mean. The computer code is steady elliptic and the numerical solution proceeds iteratively. A 140^2 mesh in the $(r,\ z)$ frame proved to be sufficient in the case considered in the present work to get grid-independent solutions. The mesh is refined close to the walls: the size of the first mesh is indeed $6.89 \times 10^{-5}H$ and $7.526 \times 10^{-4}H$ in the radial and axial directions respectively. At the wall, all the variables are set to zero except for the tangential velocity V_θ, which is set to Ωr on rotating walls and zero on stationary walls and the dissipation rate of the turbulence kinetic energy which has a finite value on all walls. In the radial gap between the stator and the hub, V_θ is supposed to vary linearly from zero on the stationary wall up to Ωr on the rotating wall. To model the opening at the periphery of the cavity, V_θ is set to zero whereas the radial velocity component V_r is set to $-V_0$ on the upper part of the gap ($z^* = z/H > 0.5$) and $V_r = V_0$ on the lower part ($z^* < 0.5$). V_0 is fixed to 10% of the local disk velocity in agreement with the experimental results. Different boundary conditions have been tested (imposed pressure, zero radial velocity) but the present choice of boundary conditions provides the best results compared to the experimental data and especially it provides the good pre-swirl ratio, which is the crucial quantity for such flows as it will be shown in the following section. A weak level of turbulence is also imposed at the periphery of the cavity. The reader can refer to previous works by Elena and Schiestel [5] and Poncet [6] for more details.

4 Analytical solution

We recall that the flow takes place inside an annular cavity between a disk of radius R (rotor) rotating with an angular velocity Ω and a stationary disk (stator). The rotor-stator system has an axial gap H and is opened at the periphery. The significant dimensionless parameters of the problem are the axial gap ratio of the cavity G, the global Reynolds number Re and the Ekman number Ek. The authors assumed that $G \ll 1$, $Re \gg 1$ and $Ek \ll 1$, which corresponds to the turbulent flow regime with separated boundary layers [3].

Following the theoretical approach by Debuchy et al. [10], valid inside the central core flow, under assumptions of incompressible, steady and axisymmetric flow with negligible turbulence effects, the momentum equations, written in dimensionless form, are reduced to:

$$\frac{\partial P^*}{\partial z^*} = 0; \quad r^* V_\theta^{*2} = \frac{1}{2}\frac{\mathrm{d}P^*}{\mathrm{d}r^*}; \quad P - P_{atm} = \frac{1}{2}\rho\Omega^2 R^2 P^* \tag{2}$$

The relevant conclusion is that the dimensionless pressure P^* and tangential velocity V_θ^* are independent of z^* inside the central core, but no analytical solution can be deduced from relation (2).

Additional relations can be provided starting from the dimensionless flow rate circulating inside the boundary layers estimated according to Owen and Rogers [12] with a weighting function as introduced by Debuchy et al. [13]. The centrifugal dimensionless flow rate inside the rotor boundary layer q_R^* must be counterbalanced by a dimensionless compensation flow rate q_C^*. For a rotor-stator system with a superimposed radial inflow, Debuchy et al. [13] suggested that the dimensionless compensation flow rate q_C^* is proportional to $(\mathrm{e}^{\varphi C q_r} K\, r^{*2} Re)^{4/5}$, with the Cq_r parameter defined by Poncet et al. [7]. In the absence of any superimposed flow, there is also a possible radial exchange inside the central core with the consequence that the Cq_r parameter has to be replaced by a pseudo-dimensionless coefficient of flow rate $\tilde{C}q_r$:

$$q_R^* \propto (r^{*2} Re)^{4/5}; \quad q_C^* \propto (\mathrm{e}^{\varphi\, \tilde{C} q_r} K\, r^{*2} Re)^{4/5} \tag{3}$$

In the present work, it is assumed that the pseudo-dimensionless coefficient of flow rate $\tilde{C}q_r$ is linked to the difference between the effective core swirl coefficient K and the core swirl coefficient corresponding to the solid body rotation K_B, and also to the dimensionless radius. Consequently, assuming that $\tilde{C}q_r \propto (K_B - K)\, r^{*a}$, and introducing the boundary condition $K = K_p$ at $r^* = 1$, it is found that:

$$\frac{K}{K_B} = \left(\frac{K_p}{K_B}\right)\left(\frac{K_B - K}{K_B - K_p}\right)^{r^{*\,a}} \tag{4}$$

The solution $K = K_B$ corresponding to a central core rotating as a solid body is obtained in the particular case

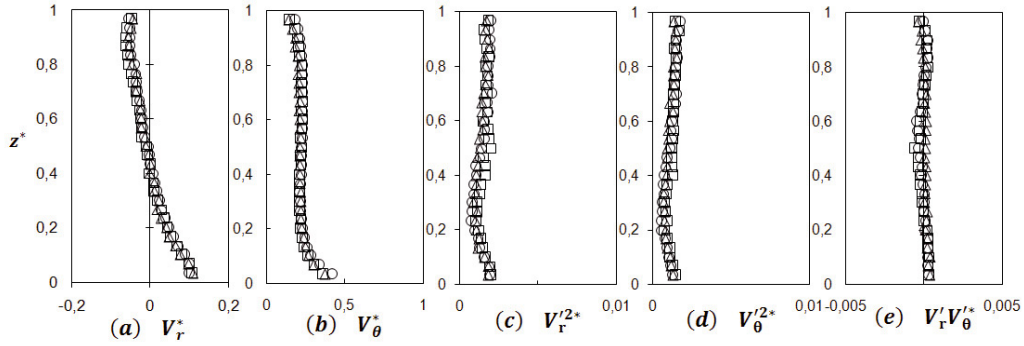

Fig. 2. Experimental results at $r^* = 0.976$. Shrouded rotor system: (o) $\lambda = 0$, (□) $\lambda = 0.27$; Unshrouded rotor system: (Δ) $\lambda = 0.27$.

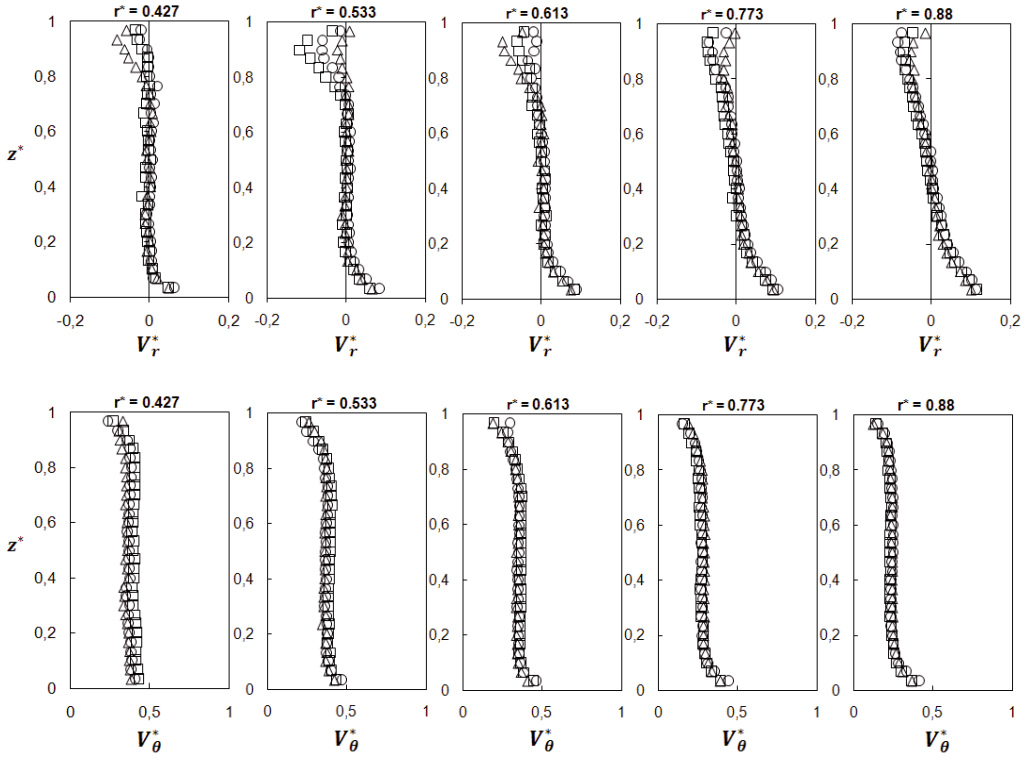

Fig. 3. Axial profiles of the mean radial and tangential velocity components at various radii. See legend of Figure 2.

$K_p = K_B$. An iterative procedure is proposed by the authors to approximate the solution for K with $K_p \neq K_B$. The domain is divided into a uniform grid with a mesh size Δr^* sufficiently small to assume that $\tilde{C}q_{r_i}$ is quasi-invariant (Fig. 1). K_{i+1} at the radial location r^*_{i+1} is computed from relation (5) using the value of K_i at the radial location $r^*_i = r^*_{i+1} + \Delta r^*_i$. This step by step process starts at $r^*_0 = 1$, where the pre-swirl coefficient is K_p. The dimensionless static pressure P^*_i at the radial location r^*_i is obtained using the following equivalent difference quotient instead of the second relation in (3), the origin of the dimensionless static pressure being $P^*_0 = 0$ at $r^*_0 = 1$:

$$\frac{K_{i+1}}{K_B} = \left(\frac{K_p}{K_B}\right)\left(\frac{K_B - K_i}{K_B - K_p}\right)^{r_i^{*\,a}} \qquad (5)$$

5 Results and discussion

The first step of the discussion is based on experimental results corresponding to three distinct geometrical configurations: two values of λ are tested ($\lambda = 0$ and $\lambda = 0.27$) in the case of a shrouded rotor system whereas only the case $\lambda = 0.27$ is retained in the case of an unshrouded rotor system. These configurations are interesting because they lead to similar peripheral conditions as depicted in Figure 2: at $r^* = 0.976$, both tangential and radial dimensionless velocity profiles as well as the corresponding turbulent correlations are superimposed. The probable reason is that the external flow structure, and consequently the peripheral inlet/outlet fluid exchange are identical for both configurations. Figure 2 shows that, at this radial location $r^* = 0.976$, the radial velocity

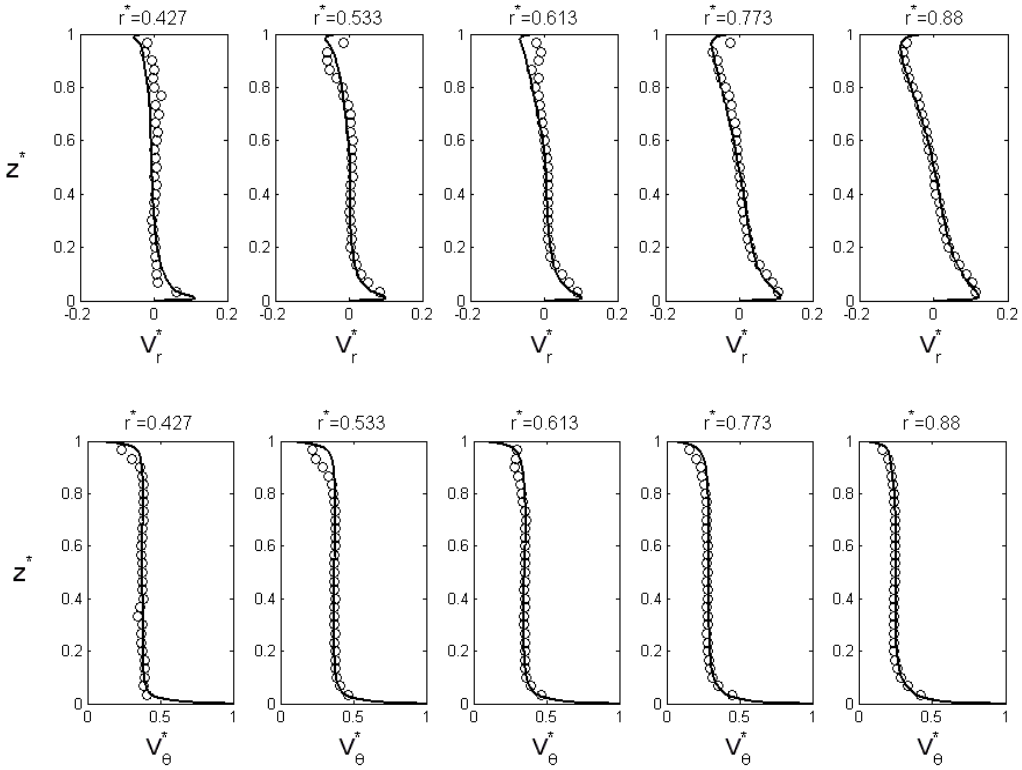

Fig. 4. Axial profiles of the mean radial and tangential velocity components. Comparison between experiments (o) and numerical results (lines).

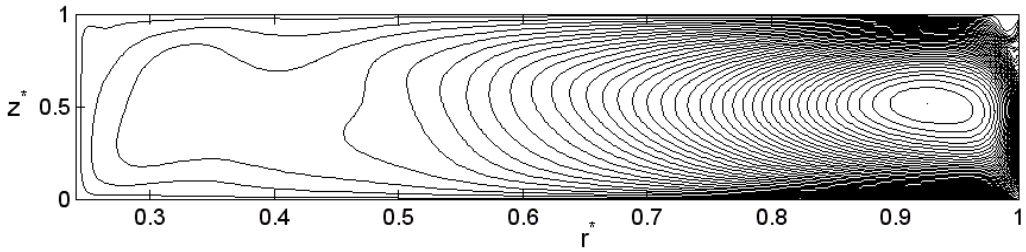

Fig. 5. Streamline patterns obtained from the numerical results.

profile is divided into two zones: the flow is directed inward on the stator side for $0.5 \leq z^* \leq 1$ and it is ejected under the centrifugal effects of the rotating wall for $z^* \leq 0.5$. It means that a radial circulation outside the boundary layers does exist. Figure 2b reveals that the tangential velocity profile is divided into three distinct zones: the two boundary layers adjacent to the disks in which the axial gradients of the velocity components are important because of the adherent conditions to the walls and a central core in which the tangential velocity is nearly independent of the axial position z. Note that the level of the pre-swirl ratio (i.e. the dimensionless tangential velocity at $r^* = 0.976$ and $z^* = 0.5$) is around 0.22. Figures 2c–2e show that the turbulence intensities are very weak.

Figure 3 brings to light that for $r^* = 0.773$, the radial velocity profiles are again divided into two zones whereas the radial exchange of fluid in the core region gradually vanishes as the local radius decreases. For $r^* = 0.613$, the radial flow circulates only through the boundary layers. The tangential velocity profile is divided into three distinct zones, as previously described, for all radii in the range $0.427 \leq r^* \leq 0.88$. The level of the dimensionless tangential velocity in the central core is a decreasing function of r^* as if there is a centripetal superimposed flow, until it reaches a nearly constant value for $r^* \leq 0.533$: the central core flow rotates as a solid body with a velocity approximately equals to 38–40% of the local velocity of the rotating disk.

The second step of the discussion deals with comparison between experiments and numerical results. As the three different geometry arrangements at the periphery of the cavity give nearly the same flow properties, the numerical results have been compared only to experimental data in the unshrouded case for $\lambda = 0.27$. Figure 4 shows comparisons for the mean radial and tangential velocity components for radii in the range $0.427 \leq r^* \leq 0.88$. The RSM model reproduces well the flow structure especially

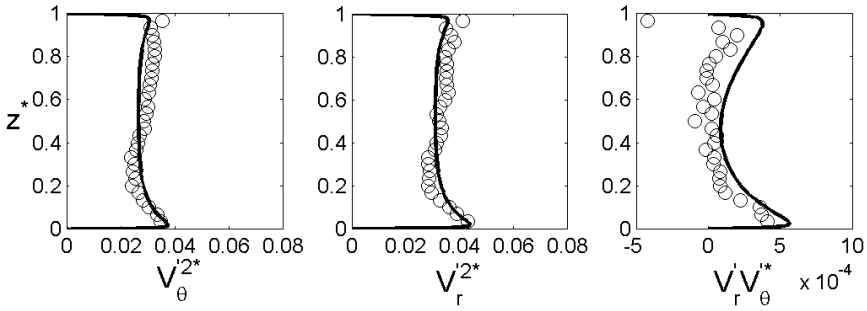

Fig. 6. Axial profiles of three components of the Reynolds stress tensor at $r^* = 0.773$. Comparison between experiments (o) and numerical results (lines).

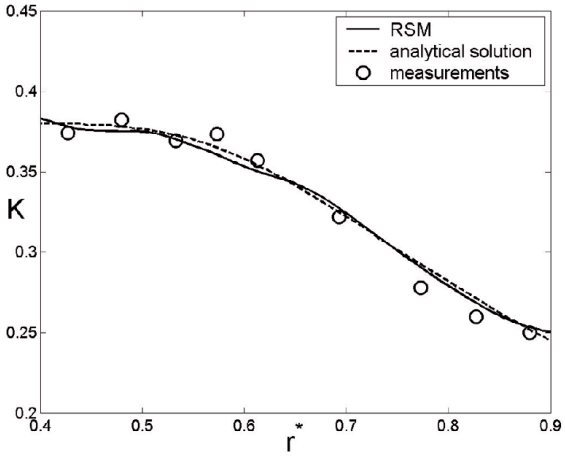

Fig. 7. Radial distributions of the core swirl ratio. Comparison between experiments (o) numerical results (line) and theory (dashed line).

at the periphery of the cavity. The tangential velocity profile is divided into three distinct zones for all values of r^*, whereas the radial velocity profile is divided into two zones near the periphery at $r^* = 0.88$, and into three zones closer to the rotation axis. When r^* decreases, note the transition to the Batchelor flow structure for $r^* \leq 0.6$, both visible in the experimental data and in the numerical results. There is an excellent agreement between the two approaches for the mean field. The Ekman layer along the rotor is well reproduced by the model as well as the core swirl ratio. A small discrepancy is observed along the stator, where the RSM model tends to underestimate the thickness of the Bödewadt layer.

Figure 5 presents the corresponding streamline patterns in a (r, z) plane. It can be seen that the secondary flow is clearly affected by the opening to the atmosphere at the periphery of the cavity with a small recirculation at the corner between the outer opening and the stator as well as large recirculation bubbles close to the walls for $r^* \geq 0.8$. Closer to the rotation axis $r^* \leq 0.5$, the flow structure resembles the Batchelor flow structure. The streamlines confirm that a radial circulation outside the boundary layers does exist, as already observed from the mean radial velocity profiles (Figs. 2, 3, 5).

The numerical results are compared to the velocity measurements for the three associated Reynolds stress components at one radial location $r^* = 0.773$ (Fig. 6). The cross component is quite weak compared to the two normal components. Turbulence is mainly concentrated in the boundary layers but, contrary to the case of turbulent flows in a closed cavity, the central core is turbulent too. Thus, turbulence intensities slightly vary with the axial position. The RSM model predicts quite well the turbulent field apart very close to the stator, where the normal turbulence intensities are slightly underestimated. These weak discrepancies may be attributed to both the difficulty to acquire measurements close to this wall but also to the choice of the boundary conditions at the periphery of the cavity in the modeling.

Figure 7 presents the radial distributions of the core swirl ratio. The theoretical distribution is deduced from formula (5) with $K_B = 0.382$, $K_p = 0.22$, $a = 0.6$ for a constant value of Δr_i^* equal to 0.005 and it is in good agreement with the numerical results and the velocity measurements for this range of radial location. The dimensionless tangential velocity level in the central core increases when approaching the rotation axis to reach a value close to 0.382 for $r^* = 0.4$. It is to be compared to the value 0.438 obtained experimentally and analytically by Poncet et al. [7] for turbulent flows in an enclosed cavity. This variation can be clearly attributed to the opening at the periphery, which strongly modifies the inlet/outlet conditions and especially the level of the core swirl ratio, which is around 0.24 for $r^* = 0.9$ in the RSM model, very close to that obtained for the unshrouded rotor cavity for the ($\lambda = 0.27$) case.

6 Conclusion

Measurements and theoretical and numerical modelings of the turbulent flow in a rotor-stator cavity are a great challenge even more when the cavity is opened to the atmosphere at the periphery. In the present work, we have compared extensive velocity measurements for configurations leading to the same value of the pre-swirl ratio equal to 0.22 and to very weak turbulence intensities around the opening. The experimental results have been used as boundary conditions in the numerical modeling.

The second order model results agree well with the experimental data for both the mean and turbulent fields. The thicknesses of the boundary layers as well as the core swirl ratio are well predicted at all radial locations. A weak discrepancy is observed along the stator, where the RSM model slightly under predicts the Bödewadt boundary layer thickness. The radial distribution of the core swirl ratio K is also well predicted by a new analytical solution valid in the central core. The main result of this work is that the flow structure and especially the core swirl ratio, which is the most interesting quantity for turbomachinery application, depend exclusively on the preswirl ratio and on the weak inward/outward radial flow at the opening.

References

[1] G.K. Batchelor, Note on a class of solutions of the Navier-Stokes equations representing steady rotationally-symmetric flow, J. Mech. Appl. Math. 4 (1951) 29–41

[2] K. Stewartson, On the flow between two rotating coaxial discs, Proc. Camb. Phil. Soc. 49 (1953) 333–341

[3] J.W. Daily, R.E. Nece, Chamber dimension effects on induced flow and frictional resistance of enclosed rotating disks, ASME J. Basic Eng. 82 (1960) 217–232

[4] M. Itoh, Y. Yamada, S. Imao, M. Gonda, Experiments on turbulent flow due to an enclosed rotating disk, Proc. Int. Symp. On Engineering Turbulence Modeling and Experiments, in: W. Rodi, E.N. Galic (éd.), Elsevier, New-York, 1990, pp. 659–668

[5] L. Elena, R. Schiestel, Turbulence modelling of rotating confined flows, Int. J. Heat Fluid Flow 17 (1996) 283–289

[6] S. Poncet, Ecoulements de type rotor-stator soumis à un flux axial : de Batchelor à Stewartson, Ph.D. thesis, University of Aix-Marseille 1

[7] S. Poncet, M.P. Chauve, P. Le Gal, Turbulent Rotating Disk Flow with Inward Throughflow, J. Fluid Mech. 522 (2005a) 253–262

[8] S. Poncet, M.P. Chauve, R. Schiestel, Batchelor versus Stewartson flow structures in a rotor-stator cavity with throughflow, Phys. Fluids 17 (2005b) 075110

[9] M. Djaoui, A. Malesys, R. Debuchy, Mise en évidence expérimentale de la sensibilité de l'écoulement de type rotor-stator aux effets de bord, C.R. Acad. Sci. Paris Série II b 327 (1998) 49–54

[10] R. Debuchy, S. Della Gatta, E. D'Haudt, G. Bois, F. Martelli, Influence of external geometrical modifications on the flow behavior of a rotor-stator system: numerical and experimental investigation, Proceedings of the I MECH E Part A Journal of Power and Energy 221 (2007) 857–863

[11] B.E. Launder, D.P. Tselepidakis, Application of a new second-moment closure to turbulent channel flow rotating in orthogonal mode, Int. J. Heat Fluid Flow 15 (1994) 2–10

[12] J.M. Owen, R.H. Rogers, Flow and heat transfer in rotating-disc system: Rotor-stator system, W.D. Morris (éd.), John Wiley & Sons Inc, Vol. 1, 1989

[13] R. Debuchy, F. Abdel Nour, G. Bois, On the flow behavior in rotor-stator system with superposed flow, International Journal of Rotating Machinery, doi:10.1155/2008/719510